2-Aminopurine Excited State Electronic Structure Measured by Stark Spectroscopy

ARTICLE *in* THE JOURNAL OF PHYSICAL CHEMISTRY B · MARCH 2008

Impact Factor: 3.3 · DOI: 10.1021/jp076374x · Source: PubMed

4 AUTHORS:

Goutham Kodali
University of Pennsylvania
30 PUBLICATIONS **152** CITATIONS
SEE PROFILE

Kurt A Kistler
Pennsylvania State University
28 PUBLICATIONS **426** CITATIONS
SEE PROFILE

Spiridoula Matsika
Temple University
73 PUBLICATIONS **1,440** CITATIONS
SEE PROFILE

Robert J Stanley
Temple University
47 PUBLICATIONS **963** CITATIONS
SEE PROFILE

2-Aminopurine Excited State Electronic Structure Measured by Stark Spectroscopy

Goutham Kodali, Kurt A. Kistler, Spiridoula Matsika, and Robert J. Stanley*

Department of Chemistry, Temple University, Philadelphia, Pennsylvania 19122

Received: August 8, 2007; In Final Form: November 6, 2007

2-Aminopurine (2AP) is an adenine analogue that has a high fluorescence quantum yield. Its fluorescence yield decreases significantly when the base is incorporated into DNA, making it a very useful real-time probe of DNA structure. However, the basic mechanism underlying 2AP fluorescence quenching by base stacking is not well understood. A critical element in approaching this problem is obtaining an understanding of the electronic structure of the excited state. We have explored the excited state properties of 2AP and 2-amino,9-methylpurine (2A9MP) in frozen solutions using Stark spectroscopy. The experimental data were correlated with high level ab initio (MRCI) calculations of the dipole moments, $\vec{\mu}_0$ and $\vec{\mu}_1$, of the ground and excited states. The magnitude and direction of the dipole moment change, $\Delta\vec{\mu}_{01} = \vec{\mu}_1 - \vec{\mu}_0$, of the lowest energy optically allowed transition was determined. While other studies have reported on the magnitude of the dipole moment change, we believe that this is the first report of the direction of $\Delta\vec{\mu}$, a quantity that will be of great value in interpreting absorption spectral changes of the 2AP chromophore. Polarizability changes due to the transition were also obtained.

Introduction

2-Aminopurine (2AP, Scheme 1) is an adenine analogue that has found extensive use as a site-specific probe of the local structure of DNA and RNA. 2AP has a high fluorescence quantum yield (0.68 in water).[1] Its optical absorption and emission transitions are well red shifted compared to the natural nucleic acid bases, and it can be selectively excited and detected. 2AP can be inserted into DNA without significantly perturbing its double helical base stacked structure.[2−5] It is used as a conformational probe in DNA binding proteins to understand the mechanism of binding.[6−13] 2AP is also used as a specific inhibitor for double stranded RNA dependent protein kinase (PKR).[14,15]

Because of its importance as an optical probe, Holmen et al. have measured the transition dipole moment of 2AP, $\vec{m}_{01}$, at ∼308 nm, by linear dichroism spectroscopy.[16] This is the transition which is usually probed to take the advantage of the 2AP chromophore as a DNA base analogue of adenine. $\vec{m}_{01}$, a vector, is extremely useful in extending the utility of 2AP for techniques using polarized light, such as Förster energy transfer approaches.

When 2AP is base stacked in DNA, the fluorescence is quenched dramatically.[17−19] Several mechanisms have been proposed for the fluorescence quenching mechanism, including excited state charge transfer[20−22] and the presence of dark states.[20−25] However, after almost four decades of research, it is not yet clear what photophysical processes lead to quenching. Experimental studies to test these theories have led to conflicting interpretations. A recent theoretical study suggests that the presence and absence of conical intersections may be responsible for emissive properties of these molecules.[26−28] In order to understand the photophysics of fluorescence quenching, we need a better understanding of the excited state electronic structure of 2AP.

SCHEME 1: 2AP with Numbering Convention

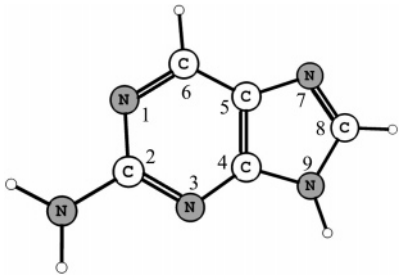

In this work, we measured the difference dipole moment, $\Delta\vec{\mu}_{01}$, and the difference polarizability, $\mathrm{Tr}(\Delta\vec{\vec{\alpha}}_{01})$, of 2AP for the $S_0 \rightarrow S_1$ transition using Stark spectroscopy. These experimental results were combined with state-of-the-art *ab initio* electronic structure calculations to elucidate the directions and magnitudes of $\Delta\vec{\mu}_{01}$, $\vec{\mu}_0$, and $\vec{\mu}_1$ in the molecular frame.

Materials and Methods

2-Aminopurine was purchased from Sigma and used as received. LiCl was purchased from Fisher Chemicals and dissolved in double-distilled deionized water to 8 M. 2-Amino,9-methylpurine (2A9MP) was synthesized from 2AP according to previously published work by Hidayatullah et al.[29] 2A9MP was purified on a silica column with an eluant mixture of chloroform/methanol/ammonia (90:10:1). It was further purified by phase separation and recrystallization in ethanol/water and characterized by ^{1}H, ^{13}C NMR, and IR spectroscopy (data not shown). 2AP and 2A9MP solutions were prepared by dissolving either 2AP or 2A9MP in 8 M LiCl solution or in 66% glycerol/water solution. The concentrations indicated below were made from 20 mM stock solutions by serial dilution.

Aqueous LiCl was used as the primary solvent for three reasons. First, it forms better low temperature optical glasses than glycerol/water does. This leads to higher quality Stark spectra. Second, we have observed that glycerol leads to

* To whom correspondence should be addressed. Phone: (215) 204-2027. Fax: (215) 204-1532.

10.1021/jp076374x CCC: $40.75
Published on Web 01/23/2008

denaturation of the DNA double strand (unpublished results) and we wish to measure the electronic properties of the monomer base in a solvent that can be used for an examination of that probe in duplex DNA. Others have shown that DNA structure is preserved at low temperature in halogenated lithium salts.[24,30]

Stark and UV−vis Absorption Spectroscopy. The basic setup of the Stark spectrometer is the same as that described previously with a few modifications.[31] A cryogenic dual reservoir nitrogen optical Dewar from JANIS Research Co was used.[32] The sample cell consists of two ITO-coated quartz slides (∼100 Ω/cm) separated by 55 μm with kapton spacers. A 20 μL portion of the sample was loaded onto one of the slides and sandwiched in a staggered manner with the other ITO-coated quartz slide, with the coatings facing each other. The cell was mounted onto a fiberglass holder with spring clips, attached to a steel rod, and plunged into the internal liquid nitrogen reservoir of the dewar.

The excitation source was a 150 W Xe arc lamp focused with a fused silica lens and filtered through a $^1/_8$ m monochromator with 2 nm band pass slits. The light was recollimated, depolarized using a calcite depolarizer, and repolarized using a Glan-Taylor polarizer. Light passing through the sample was focused onto a low noise silicon carbide (SiC) photodiode amplified by a transimpedence/instrumentation amplifier with gains of about 10^5 V/A and 10^4 V/V, respectively (Boston Electronics). The SiC signal was fed into a digital lock-in amplifier. This voltage was also digitized to 12-bit resolution to provide a measure of $I(F = 0)$. A sinusoidal AC electric field was applied to the cuvette at a frequency, ω, of 217 Hz. Phase sensitive detection of the change in the intensity of transmitted light, ΔI, with applied electric field was obtained at 2ω. Usually, nine scans were taken in equal energy steps and averaged together for a given Stark spectrum. The sample angle between the applied electric field vector and the direction of the polarized vector, χ, could be varied between ∼45 and 90°. Stark spectra were obtained at several fields and at least two different angles of χ. Six data sets were obtained for each angle of χ, and each data set was individually fitted.

Low temperature absorption spectra were obtained using the same setup by using an optical chopper and detecting the signal at $\omega = 700$ Hz. The reference for these spectra consisted of buffer in the ITO Stark cell. The buffer transmittance was taken at room temperature to avoid unnecessary scattering.

Room temperature absorption spectra were obtained on an HP8462 diode array instrument with 2 nm band pass. In some cases, low temperature spectra were measured using this instrument by inserting a Harris Martin liquid nitrogen immersion dewar in the sample compartment of the spectrometer. It should be noted that these low temperature spectra obtained with the diode array instrument were taken as a matter of convenience and were not used in the analysis of the Stark data.

Data Analysis. The analysis of Stark spectra is derived from Liptay's approach.[33,34] The low temperature Stark spectrum was obtained at the second harmonic of the AC electric field to give $\Delta I = I(F) - I(0)$. The energy-weighted field-induced change in the extinction can be given as

$$\frac{\Delta\epsilon}{\bar{\nu}} = (f\vec{F})^2\left\{\frac{A_\chi}{30\vec{m}^2}\frac{\epsilon}{\bar{\nu}} + \frac{B_\chi}{15ch}\frac{\mathrm{d}(\epsilon/\bar{\nu})}{\mathrm{d}\bar{\nu}} + \frac{C_\chi}{30c^2h^2}\frac{\mathrm{d}^2(\epsilon/\bar{\nu})}{\mathrm{d}\bar{\nu}^2}\right\} \quad (1)$$

The term $\Delta\epsilon/\bar{\nu}$ represents the energy-weighted extinction coefficient as a function of wavenumber, $\bar{\nu}$, where c is the speed of light, h is the Planck's constant, and $\vec{F}$ represents the electric field at the sample. $\Delta\epsilon/\nu$ is corrected for sample concentration, refractive index, and the χ-dependent path length. f is the field correction factor for a given solvent. We expect a field enhancement of the applied field due to the cavity field of the solvent matrix. The field correction factor is always more than one. For an ionic solution like LiCl frozen matrices, estimating the field correction factor is extremely difficult. This is discussed in more detail below.

The A_χ term is related to change in the transition moment polarizability and hyperpolarizability. In simple terms, a large change in either of these quantities might suggest that an externally applied field could induce a change in oscillator strength. We come back to this point in the Discussion section. In addition, A_χ also reflects the orientation of a dipolar molecule in response to the applied electric field. However, working in frozen media renders the sample molecules immobile, leading to a small contribution to A_χ.

Information about the change in polarizability and change in permanent dipole moment can be obtained from the B_χ and C_χ terms, respectively,[31,35,36]

$$B_\chi \sim \frac{5}{2}\mathrm{Tr}(\Delta\vec{\vec{\alpha}}) + (3\cos^2\chi - 1)\left(\frac{3}{2}\vec{m}\Delta\vec{\vec{\alpha}}\vec{m} - \frac{1}{2}\mathrm{Tr}(\Delta\vec{\vec{\alpha}})\right) \quad (2)$$

$$C_\chi = |\Delta\vec{\mu}|^2\{5 + (3\cos^2\chi - 1)(3\cos^2\zeta_A - 1)\} \quad (3)$$

where ζ_A represents angle between $\Delta\vec{\mu}$ and $\vec{m}$, the transition dipole moment. When χ is set to the magic angle (54.7°), all of the angle dependencies vanish and $\mathrm{Tr}(\Delta\vec{\vec{\alpha}})$ and $\Delta\vec{\mu}$ can be obtained directly. When this is the case, the change in the polarizability, a tensor quantity, reduces to its trace, $\mathrm{Tr}(\Delta\vec{\vec{\alpha}})$, which is a scalar representing the polarizability volume change between ground and excited states. The trace of a tensor is invariant and does not change with coordinate system. Thus, $\mathrm{Tr}(\Delta\vec{\vec{\alpha}})$ is a good estimate of the change in the polarizability.

As suggested by eq 1, this analysis requires high quality derivatives of the absorption spectrum. To this end, low temperature absorption spectra were fitted to a set of Gaussian functions. This is not a deconvolution of the absorption spectrum, but derivatives of the fitted absorption spectrum are smoother than those that can be obtained from numerical differentiation of the experimental absorption spectrum.

Although it is not necessary, the absorption spectrum and Stark spectrum were fitted simultaneously. This approach is taken precisely because the absorption spectrum derivatives are obtained from the Gaussian smoothing procedure. The Stark spectrum acts as an additional constraint on the fitted parameters. The fit was weighted equally between both of the spectra. Values are reported in terms of debyes (D) and polarizability (Å^3), where 1 D = 3.36×10^{-30} C m and 1 Å^3 = 1.113×10^{-40} C m^2 V^{-1}.

Theoretical Methods

The geometry for 2AP is the ground state minimum optimized at the MP2/6-31G(d,p) level using the Gaussian 03 suite of programs,[37] constrained to C_S symmetry. Although the true ground state minimum has C_1 symmetry, with the amino group somewhat pyramidalized, the differences in energy and dipole moment between the C_1 ground state and the C_S ground state are very small at the MP2 level, and C_S symmetry is required to carry out the more expensive *ab initio* calculations described here.

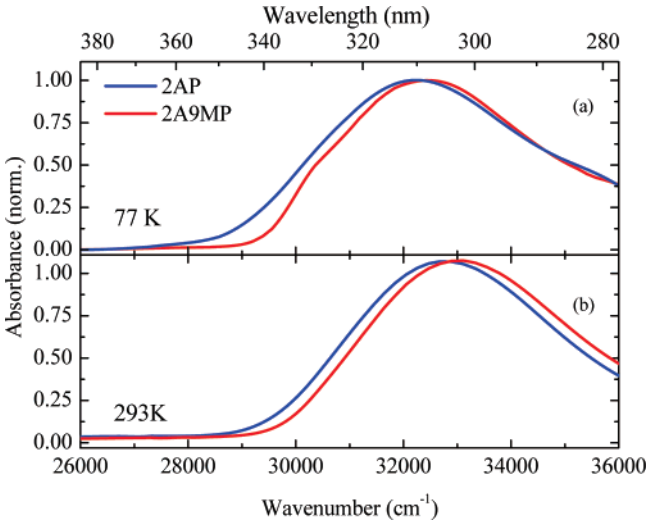

Figure 1. (a) Low temperature and (b) room temperature absorption spectra of 2AP (4.8 mM) and 2A9MP (5.0 mM) in 8 M LiCl.

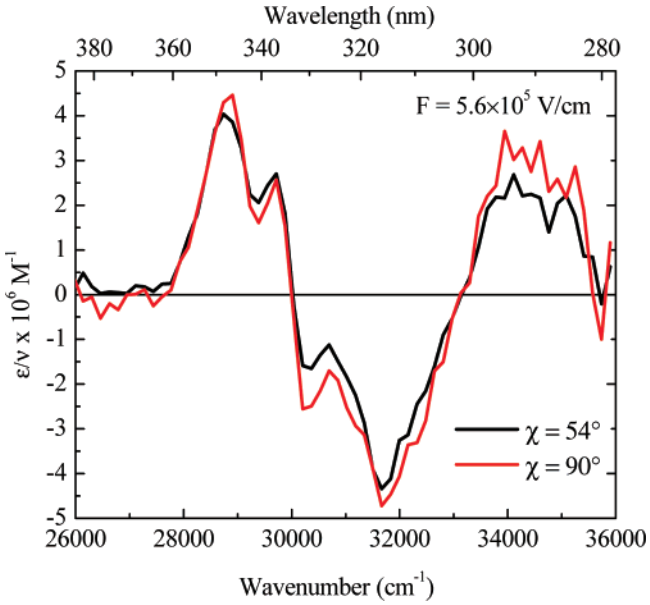

Figure 2. Stark spectra of 4.8 mM 2AP in 8 M LiCl at 77 K.

Molecular orbitals (MOs) were obtained from a state-averaged multiconfiguration self-consistent field (SA-MCSCF) procedure averaged over the first five singlet states (S_0-S_4), using Dunning's cc-pvdz atomic orbital basis set.[38] The complete active set (CAS) of orbitals included 2 n_N and 10 π orbitals, while maintaining core 1s, σ, and the remaining n_N orbital as doubly occupied. This CAS was occupied in total by 18 electrons, denoted as (18,12), where (n,m) denotes n electrons in m active orbitals. About 70000 reference configurations were generated from the SA-MCSCF calculation. These references were then used for a multireference configuration interaction (MRCI) calculation, where all core 1s and σ orbitals were maintained as frozen, and single excitations were allowed from the CAS orbitals to the virtual orbitals. This generated about 20 million configurations in the MRCI expansion, with energies, static state dipoles, and transition dipoles calculated at the MRCI level. While the SA-MCSCF calculation with this large CAS is far more expensive than a calculation done with a (12,9) or (14,10) CAS, the inclusion of all 10 π orbitals in the CAS at the MRCI level gives more accurate $\pi\pi^*$ excited state energies using the expansion described above than a much more expensive expansion previously reported for adenine.[39] That expansion included both single and double excitation configurations from a (12,9) CAS, along with single excitations from the σ orbitals, for a total of about 200 million configurations, corresponding to a calculation many times longer than the MRCI calculation described here in this report. In addition, the magnitude and orientation of the ground state dipole moment for 2AP at the MRCI level used in this report were very close to the same values calculated at the MP2 level. SA-MCSCF and MRCI calculations were carried out using the COLUMBUS Quantum Chemistry Program Suite.[40−42]

The ground state geometry of 2AP was calculated at the MP2 level on a PowerSpec Core-Duo desktop, using Gaussian 03. The MCSCF and MRCI were calculated on that MP2 geometry using Columbus, on a Dell 64-bit quad-core workstation with 8 GB of RAM. The operating system on the workstation was RedHat Linux Enterprise.

Results

The low temperature and room temperature absorption spectra of 2AP at 4.8 mM and 2A9MP at 5.0 mM in 8 M LiCl are shown in Figure 1a. To the best of our knowledge, this is the first reported low temperature absorption spectrum for both 2AP and 2A9MP. The 2AP spectrum shows one broad band, assigned to the $S_0 \rightarrow S_1$ transition, which peaks at 32230 cm^{-1} (~308 nm). This transition overlaps with $S_0 \rightarrow S_2$ on the blue side of the absorption spectrum in the ~35000 cm^{-1} region. The low temperature absorption spectrum of 2A9MP at nearly the same concentration has a maximum at 32480 cm^{-1} (~305 nm) and a shoulder at 30360 cm^{-1}. Both show some vibronic structure, which becomes more evident in the Stark spectra. 2AP and 2A9MP absorption spectra at room temperature in 8 M LiCl salt solutions are shown in Figure 1b. The room temperature absorption spectra reveals an ~440 cm^{-1} blue shift for 2AP and an ~620 cm^{-1} blue shift for 2A9MP compared to the low temperature result.

The energy-weighted Stark spectra of 2AP taken at $\chi = 54$ and 90° for $F = 3.1 \times 10^5$ V/cm are shown in Figure 2. There was almost no χ angle dependence observed in the Stark spectra. Both spectra were simultaneously fitted with the sum of zeroth, first, and second derivatives of the energy-weighted fitted absorption spectrum and the A_χ,B_χ, and C_χ parameters were obtained. The analysis of the Stark spectra was done assuming there is no contribution from the $S_0 \rightarrow S_2$ transition below 35000 cm^{-1}. The one-band fit for $\chi = 54°$ is shown in Figure 3a for comparison, along with the residuals of the fit. The individual contributions of the zeroth, first, and second derivative components are plotted in Figure 3b. Fits were also performed fixing $A_\chi = 0$, and no significant changes to B_χ and C_χ were observed.

The Stark spectrum is dominated by the second derivative component, indicating that the $S_0 \rightarrow S_1$ transition is dominated by a nonzero $\Delta\vec{\mu}$. Both zeroth and first derivatives have nonzero contributions as well, although they are smaller than the second derivative contribution. The difference dipole moments and difference polarizabilities were calculated from these fits (see Table 1). If $f = 1.4$, then $|\Delta\vec{\mu}| = 3.7$ D (±0.3) and $\mathrm{Tr}(\Delta\vec{\alpha}) = -24$ Å^3 (±20). ζ_A was about 56°.

While evidence from linear dichroism studies[16] on 2AP supports this one-band analysis, a two-band analysis was performed to see how sensitive the A_χ, B_χ, and C_χ parameters were to this assumption. The two-band analysis gave the same A_χ, B_χ, and C_χ parameters as the one-band fit for the low energy transition, within the error of the analysis (results not shown).

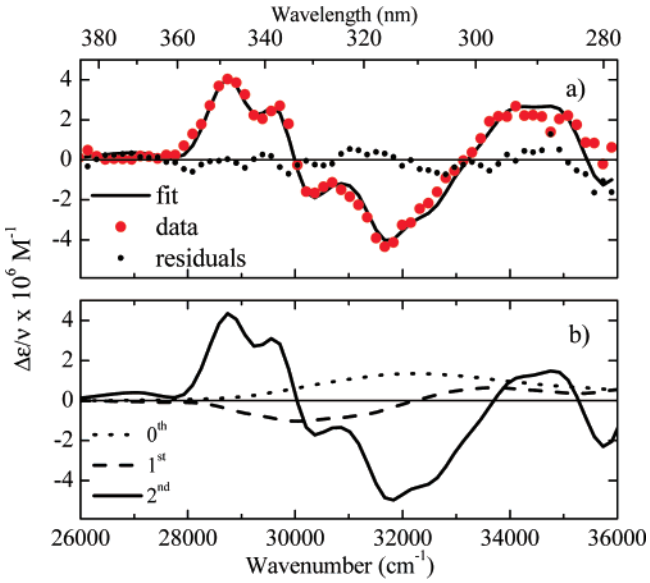

Figure 3. (a) Stark data, fit, and residuals for 4.8 mM 2AP in 8 M LiCl glass at 77 K. (b) Zeroth, first, and second derivative components of the fit.

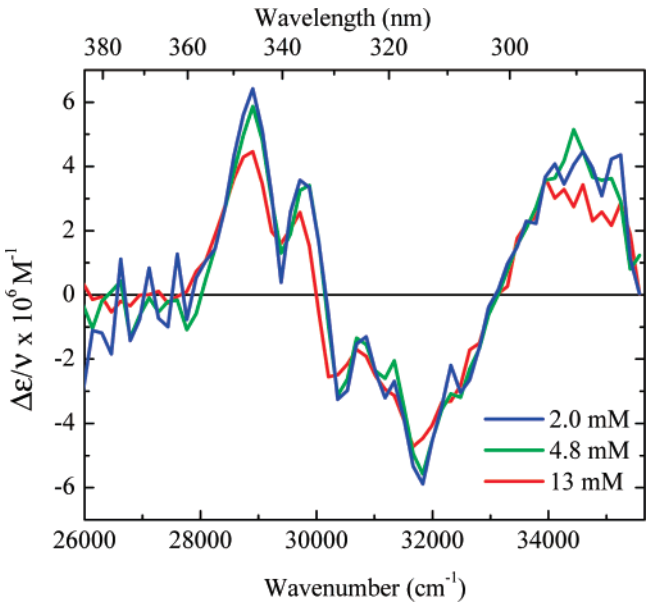

Figure 4. 2AP Stark spectra as a function of concentration.

A more significant error in the analysis might be the neglect of the effect of aggregates formed at high concentrations and low temperature on the Stark spectra. Formation of dimers and multimers is possible in aqueous solutions at high concentrations.[43,44] We have observed fluorescence quenching in 700 μM 2AP solutions, indicating that at least collisional quenching is taking place (data not shown). Stark spectra were obtained from 2−13 mM 2AP to test for aggregation (Figure 4). These spectra were normalized for concentration and field and are the same to within the signal-to-noise ratio of the data. $|\Delta\vec{\mu}_{01}|$, Tr $(\Delta\vec{\bar{\alpha}}_{01})$, and ζ_A values from fitting these data were also unchanged (see Table 1). This analysis does not rule out aggregation, but it suggests that any aggregates are weakly coupled electronically.

This is further corroborated by low temperature absorption spectra taken as a function of concentration (see Supporting Information Figure S.1). The low temperature absorption spectrum of 2-aminopurine showed a small concentration dependence from 0.6 to 20 mM. A red shift was observed with increasing concentration (a similar red shift was obtained for 2A9MP, see Supporting Information Figure S.2). Even though the concentration increased ~30-fold, the spectral shift was small, ~500 cm^{-1}. Using the 611 μM spectrum as a reference, difference spectra, $\Delta A = A[2\text{Ap}] - A_{611\mu\text{M}}$, showed evidence for an additional band growing in at around 31000 cm^{-1} (~325 nm) as a function of concentration (Supporting Information Figure S.3).

Another potential complication in the assignment of the spectra is the ability of 2AP to tautomerize between the N_9 and N_7 nitrogens. To rule out the effect of tautomerization on the Stark spectrum of 2AP, we methylated 2AP at the N9 position to make 2A9MP and measured its Stark spectrum (see Supporting Information Figure S.4). The Stark spectrum looks sharper than the 2AP Stark spectrum due to the better resolved vibronic structure in the low temperature absorption spectrum (Figure 1a), but an analysis of the Stark spectrum yielded almost the same parameters as for 2AP: $|\Delta\vec{\mu}_{01}| = 4.1$ D (±0.4), Tr$(\Delta) = -29$ Å^3 (±16), and $\zeta_A = 62°$ (±6), ruling out tautomerism in the interpretation of the 2AP results.

Stark spectra were obtained in 66% glycerol/33% water to test the effect of solvent on the electronic structure parameters. This glass not only has a different f value but is nonionic, unlike LiCl which could alter the cavity electric field significantly and potentially modulate the electronic structure distribution. The Stark spectrum did not change in the glycerol/water glass relative to that of 2AP in LiCl (Supporting Information Figure S.5), and an analysis gives almost the same values within experimental error (see Table 1).

The direction of $\Delta\vec{\mu}_{01}$ was obtained relative to the transition dipole moment direction for $S_0 \rightarrow S_1$ transition, $\vec{m}_{01}$, as determined from LD spectroscopy of 2AP in PVA films.[16] The angle between the transition dipole moment and the difference dipole moment, ζ_A, was obtained from the analysis of Stark spectra taken at two different angles of χ. The direction of $\vec{\mu}_1$ was calculated by combining the MRCI-calculated ground state dipole moment direction with the experimentally determined direction and magnitude of $\Delta\vec{\mu}_{01}$. The MRCI value of $\vec{\mu}_0$ was 3.24 D in the gas phase, which agreed quite well with other calculated values (see Table 2). The experimental difference dipole, however, is not a gas phase value. Therefore, we scaled the gas phase MRCI ground state dipole magnitude guided by a CIS calculation of 2AP, which gave 3.22 D in the gas phase

TABLE 1: Electronic Structure Parameters for 2AP and 2A9MP ($f = 1.4$)

	$\lvert\Delta\vec{\mu}_{01}\rvert$ (D)	Tr$(\Delta\vec{\bar{\alpha}}_{01})$ (Å^3)	ζ_A (deg)
2 mM 2AP[a]	3.7 ± 0.3	−24 ± 20	54 ± 9
4.8 mM 2AP[a]	3.6 ± 0.4	−31 ± 24	56 ± 4
13 mM 2AP[a]	3.6 ± 0.3	−26 ± 32	54 ± 2
5 mM 2AP[b]	4.2 ± 0.3	−28 ± 16	59 ± 3
5.3 mM 2A9MP[a]	4.1 ± 0.4	−29 ± 21	62 ± 6

[a] 8 M LiCl. [b] 66% glycerol/H_2O.

TABLE 2: Computational Data

method	molecule	$\lvert\vec{\mu}_0\rvert$	$\lvert\vec{\mu}_1\rvert$	$\angle\vec{\mu}_0,\vec{\mu}_1$ (deg)	$\lvert\vec{\Delta}\mu_{01}\rvert$
MRCI[a]	2AP	3.24	4.22	17	1.5
CASPT2[b]	2AP	3.32	3.24	8.9	0.5
MCSCF/solvatochromism[c]	2A9MP	3.60	4.60		
CASSCF (10,14 CAS)[d]	2A9MP	3.64	4.68	24	2.0
CIS(gas phase)[e]	2AP	3.22	4.49	21	1.9
CIS(SCRF/water)[e]	2AP	4.50	6.18	11	2.0

[a] This work. [b] Perun et al.[26] [c] Rachofsky et al.[59] [d] Rachofsky et al.[48] [e] Jean et al.[45]

SCHEME 2: Electronic Structure of 2AP[a]

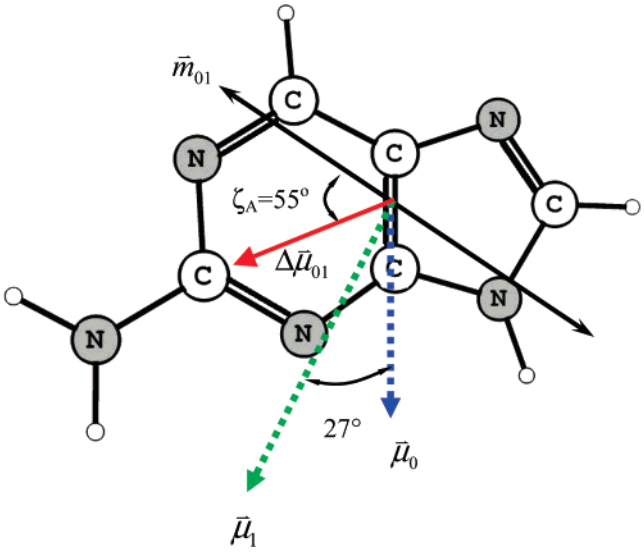

[a] $|\Delta\mu_{01}| = 3.6$ D, $|\mu_0| = 4.5$ D, $|\mu_1| = 6.8$ D.

and 4.5 D in water using a continuum dielectric solvation approximation.[45] Thus, the value of $\vec{\mu}_1$ in solvent was obtained by requiring that its direction give the Stark-derived magnitude and direction of $\Delta\vec{\mu}_{01}$ in relation to $\vec{\mu}_0 = 4.5$ D (see Supporting Information Figure S.6). This approach makes $\angle\vec{\mu}_0,\vec{\mu}_1 = 27°$ and $|\vec{\mu}_1| = 6.8$ D.

On the basis of these calculations, the directions of the difference dipole moment and excited state dipole moment were assigned relative to the $S_0 \rightarrow S_1$ transition dipole and are shown superimposed on the 2AP framework in Scheme 2. Interestingly, the ground state dipole moment is aligned parallel to the short molecular axis defined by the C_4-C_5 axis and $\Delta\vec{\mu}_{01}$ is oriented approximately along the 2-amino position. $\vec{\mu}_1$ points almost midway between these two vectors. To our knowledge, this is the first determination of the direction of $\Delta\vec{\mu}_{01}$ and $\vec{\mu}_1$ in 2AP, based on experimental data.

Discussion

We have obtained $\Delta\vec{\mu}$, $\mathrm{Tr}(\Delta\vec{\alpha})$, and the dipole moment angles for the lowest energy optically allowed transition in 2AP and 2A9MP for the first time using Stark spectroscopy. These values appear to be independent of concentration, tautomerization, and solvent polarity at this level of accuracy. The magnitude of $\Delta\vec{\mu}$ is consistent with all other previously reported experimental values given in the literature.[2,46,47] The directions of $\Delta\vec{\mu}$ and $\vec{\mu}_1$ were consistent with theoretical calculations from this work and previous theoretical studies.[45,48]

Tautomerization might play a role in the observed Stark spectra. Previous studies showed that the 9-H tautomer is more stable than the 7-H tautomer.[49] An analysis of Stark spectra of 2A9MP gave the same results as those for 2AP. However, in 2A9MP, the 7-H tautomer cannot be formed. This suggests that the 7-H tautomer is not significantly populated in 2AP at low temperature.

The concentration-dependent spectral shift appears to be due to the stacking of 2AP molecules. However, the spectral shift is very small ($\sim$600 cm^{-1}). This kind of spectral shift was previously reported in DNA duplexes where two 2AP molecules are adjacent to each other[50] as well as in 2AP crystals.[51] However, in 2AP-containing DNA where the 2AP bases are stacked in a head-to-head orientation the absorption spectrum is blue shifted,[52] the opposite of our observations for the monomer in free solution. In order to explain the red shift observed in our case, the 2AP bases have to be stacked in head-to-tail fashion. We anticipate that head-to-tail stacked dimers form readily, with the monomers oriented so that their ground state dipole moments are antiparallel. This orientation puts the transition dipole moments of the monomers at an angle of about 60°, because the transition dipole moment is not parallel to the ground state dipole moment. There might be a distribution of geometries in which the average dihedral angle between transition dipole moments of two monomers lies between 54 and 90°.

The absolute value of $\Delta\vec{\mu}$ and $\mathrm{Tr}(\vec{\alpha})$ depends on f, the local field correction factor, which for LiCl solution is difficult to estimate. The dielectric constant and refractive index are rarely published for compounds at cryogenic temperatures. The dielectric constant for LiCl solution reported at 200 K for 8 M concentration is $\epsilon = 15$.[53] Using this dielectric constant, the field correction factor was estimated to be $f = 1.4$ using a spherical cavity reaction field method. For water/glycerol, the field correction factor was estimated as 1.25.[36] Usually field correction factors lie between 1.1 and 1.4.[35,54] The values for $\Delta\vec{\mu}$ and $\mathrm{Tr}(\Delta\vec{\alpha})$ derived from LiCl glasses shown in Table 1 are corrected for $f = 1.4$.

Interestingly, the value for A_χ was small. This suggests that changes in the transition moment (hyper)polarizibility are also small, ruling out a role for an external electric field to modulate the oscillator strength of 2AP. This, in turn, suggests that fluorescence quenching of excited 2AP is probably not due to dipolar solvent effects. In particular, the dipolar electric field presented by neighboring bases in a DNA duplex, while important for hypochromism, may not be a large factor for 2AP quenching that accompanies duplex formation.

Comparison of our results for 2AP with Stark spectra for adenine yielded similar results in the magnitude of the difference dipole moment ($|\Delta\vec{\mu}|$) and difference polarizability ($\mathrm{Tr}\Delta\vec{\alpha}$). The difference dipole moment for $S_0 \rightarrow S_1$ transition in adenine is 3.2 D,[55] whereas the difference polarizability is +43 $Å^3$. In both cases, the difference polarizability is small. $\Delta\vec{\mu}$ in both cases is directed toward the amino group. The amino groups in 2AP and adenine (6-aminopurine) are roughly perpendicular to each other. The angle between the transition dipole moment and the difference dipole moment changed by 15° in 2AP ($\zeta_A \sim 55°$), when compared to adenine ($\zeta_A \sim 40°$).[55] The lack of a large difference in the electronic structure parameters of 2AP versus adenine determined by absorption Stark spectroscopy suggests that the excited state reached upon absorption of a photon is not very different for 2AP compared to adenine. However, the fact that excited state lifetimes and emission yields are so different points to large changes that must occur after the absorption event. Current theoretical treatments of the fate of excitation energy in nucleic acid bases and their analogues suggests that the Franck−Condon excited state of adenine evolves to a lower energy state that finds a conical intersection leading to excited state relaxation and low fluorescence.[39,56−58] On the contrary, the lowest $\pi \rightarrow \pi^*$ transition in 2AP leads to a conical intersection, but the excited molecule must overcome an $\sim$5−10 kcal/mol barrier to access it,[26−28] so that the excitation energy is subsequently lost through high yield emission of a fluorescence photon.

This work has resulted in a determination of both the magnitude and direction of the excited state absorption dipole moment of the optically accessible state used by many researchers to probe DNA structural dynamics by steady state and time-resolved spectroscopies. This new information will make it

possible to correlate spectral shifts of the 2AP chromophore in duplex DNA due to the identity and orientation of neighboring bases. For a given configuration, the overall vectorial electric field, $\vec{F}$, produced by dipolar nucleic acid bases surrounding 2AP will shift the transition energy, ΔE. The degree of change will depend on both the direction of $\Delta\vec{\mu}$, and its magnitude, such that $\Delta E = -\Delta\vec{\mu}\cdot\vec{F}$. We can imagine that carefully designed single molecule microscopy experiments will be able to measure these configuration-dependent spectral shifts on duplexes such that dynamical and structural information will be extracted about the relative motions of bases surrounding the fluorescent probe. This should lead to greater insights into the role of dynamics and sequence in the study of nucleic acid structure and protein: DNA/RNA interactions in real time.

Conclusion

The difference dipole moment, $\Delta\vec{\mu}$, difference polarizability, $\mathrm{Tr}(\Delta\vec{\vec{\alpha}})$, and angle between the difference dipole moment and transition dipole moment, ζ_A, were experimentally determined using Stark spectroscopy. These values allowed us to calculate the direction of difference dipole moment and lowest excited state dipole moment directions in the molecular frame of reference based on the experimental transition dipole moment direction[16] and the MRCI-calculated ground state dipole moment direction. The difference polarizabilities were measured for 2AP for the first time. The increase in dipole moment from ground state to first excited state is in agreement with other experimental and theoretical studies. The magnitude of difference dipole moment did not change significantly compared to adenine except for its direction. This change in the direction of difference dipole moment, which represents the net change in the charge redistribution from 2AP to that of adenine, might explain the different photophysics of 2AP when compared to the other naturally occurring nucleic acid bases. There might be a significant difference in relaxed excited or emitting state between 2AP and adenine, which could explain the abnormal fluorescence properties of 2AP. Electroemission studies are underway in our laboratory to look at the emitting state electronic properties of 2AP.

Acknowledgment. The authors wish to thank Sushmita Sen and Ramakrishna Edupuganti for help in synthesizing the 2A9MP, Mr. Alexander Babich for discussions regarding the geometry of 2AP, and Professor Ed Castner for useful discussions regarding ionic liquids. G.K. and R.J.S. are grateful for support from the NSF Molecular Biosciences Division (MCB-0347087). K.A.K. and S. M. received support from NSF CHE-0449853.

Supporting Information Available: Five spectra and one graph are available. These data show the concentration dependence of the absorption spectra for the 2AP and 2A9MP chromophores. The Stark spectra for 2A9MP in LiCl and 2AP in glycerol/water are also included. The dependence of the angle and excited state dipole moment on the ground state dipole moment is also shown. This material is available free of charge via the Internet at http://pubs.acs.org.

References and Notes

(1) Ward, D. C.; Reich, E.; Stryer, L. *J. Biol. Chem.* **1969**, *244*, 1228.
(2) Evans, K.; Xu, D.; Kim, Y.; Nordlund, T. M. *J. Fluoresc.* **1992**, *2*, 209.
(3) Nordlund, T. M.; Xu, D.; Evans, K. O. *Biochemistry* **1993**, *32*, 12090.
(4) Nordlund, T. M.; Xu, D.; Evans, K. O. *Proc. SPIE-Int. Soc. Opt. Eng.* **1994**, *2137*, 634.
(5) Xu, D.; Evans, K. O.; Nordlund, T. M. *Biochemistry* **1994**, *33*, 9592.
(6) Nordlund, T. M.; Andersson, S.; Nilsson, L.; Rigler, R.; Graeslund, A.; McLaughlin, L. W. *Biochemistry* **1989**, *28*, 9095.
(7) McCullough, A. K.; Dodson, M. L.; Scharer, O. D.; Lloyd, R. S. *J. Biol. Chem.* **1997**, *272*, 27210.
(8) Allan, B. W.; Reich, N. O. *Biochemistry* **1996**, *35*, 14757.
(9) Yang, K.; Stanley, R. J. *Biochemistry* **2006**, *45*, 11239.
(10) Hariharan, C.; Reha-Krantz, L. J. *Biochemistry* **2005**, *44*, 15674.
(11) Somsen, O. J. G.; Keukens, L. B.; Niels de Keijzer, M.; van Hoek, A.; van Amerongen, H. *ChemPhysChem* **2005**, *6*, 1622.
(12) Christine, K. S.; MacFarlane, A. W. I. V.; Yang, K.; Stanley, R. J. *J. Biol. Chem.* **2002**, *277*, 38339.
(13) Bloom, L. B.; Otto, M. R.; Beechem, J. M.; Goodman, M. F. *Biochemistry* **1993**, *32*, 11247.
(14) Hosoi, T.; Matsunami, N.; Nagahama, T.; Okuma, Y.; Ozawa, K.; Takizawa, T.; Nomura, Y. *Eur. J. Pharmacol.* **2006**, *553*, 61.
(15) Hu, Y.; Conway, T. W. *J. Interferon Res.* **1993**, *13*, 323.
(16) Holmen, A.; Norden, B.; Albinsson, B. *J. Am. Chem. Soc.* **1997**, *119*, 3114.
(17) Jean, J. M.; Hall, K. B. *Proc. Natl. Acad. Sci. U.S.A.* **2001**, *98*, 37.
(18) Jean, J. M.; Hall, K. B. *Biochemistry* **2002**, *41*, 13152.
(19) Rachofsky, E. L.; Osman, R.; Ross, J. B. A. *Biochemistry* **2001**, *40*, 946.
(20) Larsen, O. F. A.; van Stokkum, I. H. M.; de Weerd, F. L.; Vengris, M.; Aravindakumar, C. T.; van Grondelle, R.; Geacintov, N. E.; van Amerongen, H. *Phys. Chem. Chem. Phys.* **2003**, *6*, 154.
(21) Wan, C.; Fiebig, T.; Schiemann, O.; Barton, J. K.; Zewail, A. H. *Proc. Natl. Acad. Sci. U.S.A.* **2000**, *97*, 14052.
(22) Fiebig, T.; Wan, C.; Zewail, A. H. *ChemPhysChem* **2002**, *3*, 781.
(23) O'Neill, M. A.; Becker, H.-C.; Wan, C.; Barton, J. K.; Zewail, A. H. *Angew. Chem., Int. Ed.* **2003**, *42*, 5896.
(24) O'Neill, M. A.; Dohno, C.; Barton, J. K. *J. Am. Chem. Soc.* **2004**, *126*, 1316.
(25) Kelley, S. O.; Barton, J. K. *Science* **1999**, *283*, 375.
(26) Perun, S.; Sobolewski, A. L.; Domcke, W. *Mol. Phys.* **2006**, *104*, 1113.
(27) Seefeld, K. A.; Pluetzer, C.; Loewenich, D.; Haeber, T.; Linder, R.; Kleinermanns, K.; Tatchen, J.; Marian, C. M. *Phys. Chem. Chem. Phys.* **2005**, *7*, 3021.
(28) Serrano-Andres, L.; Merchan, M.; Borin, A. C. *Proc. Natl. Acad. Sci. U.S.A.* **2006**, *103*, 8691.
(29) Hedayatullah, M. *J. Heterocycl. Chem.* **1982**, *19*, 249.
(30) Cai, Z.; Li, X.; Sevilla, M. D. *J. Phys. Chem. B* **2002**, *106*, 2755.
(31) Stanley, R. J.; Siddiqui, M. S. *J. Phys. Chem. A* **2001**, *105*, 11001.
(32) Andrews, S. S.; Boxer, S. G. *Rev. Sci. Instrum.* **2000**, *71*, 3567.
(33) Liptay, W. *Excited States* **1974**, *1*, 129.
(34) Liptay, W.; Walz, G.; Baumann, W.; Schlosser, H. J.; Deckers, H.; Detzer, N. *Z. Naturforsch., A* **1971**, *26*, 2020.
(35) Bublitz, G. U.; Boxer, S. G. *Annu. Rev. Phys. Chem.* **1997**, *48*, 213.
(36) Stanley, R. J.; Jang, H. *J. Phys. Chem. A* **1999**, *103*, 8976.
(37) Frisch, M. J.; Trucks, G. W.; Schlegel, H. B.; Scuseria, G. E.; Robb, M. A.; Cheeseman, J. R.; Montgomery, J. A., Jr.; Vreven, T.; Kudin, K. N.; Burant, J. C.; Millam, J. M.; Iyengar, S. S.; Tomasi, J.; Barone, V.; Mennucci, B.; Cossi, M.; Scalmani, G.; Rega, N.; Petersson, G. A.; Nakatsuji, H.; Hada, M.; Ehara, M.; Toyota, K.; Fukuda, R.; Hasegawa, J.; Ishida, M.; Nakajima, T.; Honda, Y.; Kitao, O.; Nakai, H.; Klene, M.; Li, X.; Knox, J. E.; Hratchian, H. P.; Cross, J. B.; Adamo, C.; Jaramillo, J.; Gomperts, R.; Stratmann, R. E.; Yazyev, O.; Austin, A. J.; Cammi, R.; Pomelli, C.; Ochterski, J. W.; Ayala, P. Y.; Morokuma, K.; Voth, G. A.; Salvador, P.; Dannenberg, J. J.; Zakrzewski, V. G.; Dapprich, S.; Daniels, A. D.; Strain, M. C.; Farkas, O.; Malick, D. K.; Rabuck, A. D.; Raghavachari, K.; Foresman, J. B.; Ortiz, J. V.; Cui, Q.; Baboul, A. G.; Clifford, S.; Cioslowski, J.; Stefanov, B. B.; Liu, G.; Liashenko, A.; Piskorz, P.; Komaromi, I.; Martin, R. L.; Fox, D. J.; Keith, T.; Al-Laham, M. A.; Peng, C. Y.; Nanayakkara, A.; Challacombe, M.; Gill, P. M. W.; Johnson, B.; Chen, W.; Wong, M. W.; Gonzalez, C.; Pople, J. A. *Gaussian 03*, revision C.01; Gaussian, Inc.: Pittsburgh, PA, 2003.
(38) Dunning, T. H. *J. Chem. Phys.* **1989**, *90*, 1007.
(39) Matsika, S. *J. Phys. Chem. A* **2005**, *109*, *7538*.
(40) Lischka, H.; Shepard, R.; Pitzer, R. M.; Shavitt, I.; Dallos, M.; Muller, T.; Szalay, P. G.; Seth, M.; Kedziora, G. S.; Yabushita, S.; Zhang, Z. *Phys. Chem. Chem. Phys.* **2001**, *3*, 664.
(41) (a) Lischka, H. S.; Shepard, R.; Shavitt, I.; Pitzer, R. M.; Dallos, M.; Müller, T.; Szalay, P. G.; Brown, F. B.; Ahlrichs, R.; Böhm, H. J.; Chang, A.; Comeau, D. C.; Gdanitz, R.; Dachsel, H.; Ehrhardt, C.; Ernzerhof, M.; Höchtl, P.; Irle, S.; Kedziora, G.; Kovar, T.; Parasuk, V.; Pepper, M. J. M.; Scharf, P.; Schiffer, H.; Schindler, M.; Schüler, M.; Seth, M.; Stahlberg, E. A.; Zhao, J.-G.; Yabushita, S.; Zhang, Z.; Barbatti, M.;

Matsika, S.; Schuurmann, M.; Yarkony, D. R.; Brozell, S. R.; Beck, E. V.; Blaudeau, J.-P. *COLUMBUS, an ab initio electronic structure program*, release 5.9.1, 2006. (b) Lischka, H.; Shepard, R.; Pitzer, R. M.; Shavitt, I.; Dallos, M.; Müller, Th.; Szalay, P. G.; Seth, M.; Kedziora, G. S.; Yabushita, S.; Zhang, Z. *Phys. Chem. Chem. Phys.* **2001**, *3*, 664.

(42) Lischka, H.; Shepard, R.; Brown, F. B.; Shavitt, I. *Int. J. Quantum Chem.* **1981**, *15*, 91 (Quantum Chemistry Symposium).

(43) Bierzynski, A.; Kozlowska, H.; Wierzchowski, K. L. *Biophys. Chem.* **1977**, *6*, 213.

(44) Bierzynski, A.; Kozlowska, H.; Wierzchowski, K. I. *Biophys. Chem.* **1977**, *6*, 223.

(45) Jean, J. M.; Hall, K. B. *J. Phys. Chem. A* **2000**, *104*, 1930.

(46) Smagowicz, J.; Wierzchowski, K. L. *J. Lumin.* **1974**, *8*, 210.

(47) Kawski, A.; Bartoszewicz, B.; Gryczynski, I.; Krajewski, M. *Bull. Acad. Pol. Sci., Ser. Sci., Math., Astron. Phys.* **1975**, *23*, 367.

(48) Rachofsky, E. L.; Ross, J. B. A.; Krauss, M.; Osman, R. *J. Phys. Chem. A* **2001**, *105*, 190.

(49) Ramaekers, R.; Adamowicz, L.; Maes, G. *Eur. Phys. J. D* **2002**, *20*, 375.

(50) Rist, M. J.; Marino, J. P. *Curr. Org. Chem.* **2002**, *6*, 775.

(51) Neely, R. K.; Magennis, S. W.; Parsons, S.; Jones, A. C. *ChemPhysChem* **2007**, *8*, 1095.

(52) Rist, M.; Wagenknecht, H.-A.; Fiebig, T. *ChemPhysChem* **2002**, *3*, 704.

(53) Wei, Y. Z.; Sridhar, S. *J. Chem. Phys.* **1990**, *92*, 923.

(54) Andrews, S. S. *The measurement and physics of vibrational Stark effects*; Stanford University: Stanford, CA, 2001.

(55) Luchowski, R.; Krawczyk, S. *Chem. Phys.* **2005**, *314*, 309.

(56) Kistler, K. A.; Matsika, S. *Photochem. Photobiol.* **2007**, *83*, 611.

(57) Kistler, K. A.; Matsika, S. *J. Phys. Chem.* A **2007**, *111*, 2650.

(58) Matsika, S. *Rev. Comput. Chem.* **2007**, *23*, 83.

(59) Rachofsky, E. L.; Ross, J. B. A.; Krauss, M.; Osman, R. *Acta Phys. Pol., A* **1998**, *94*, 735.